A one-dimensional collisional model for plasma-immersion ion implantation

V. Vahedi, M. A. Lieberman, M. V. Alves,[a] J. P. Verboncoeur, and C. K. Birdsall
Plasma Theory and Simulation Group, University of California, Berkeley, California 94720

(Received 20 July 1990; accepted for publication 2 November 1990)

Plasma-immersion ion implantation (also known as plasma-source ion implantation) is a process in which a target is immersed in a plasma and a series of large negative-voltage pulses are applied to it to extract ions from the plasma and implant them into the target. A general one-dimensional model is developed to study this process in different coordinate systems for the case in which the pressure of the neutral gas is large enough that the ion motion in the sheath can be assumed to be highly collisional.

I. INTRODUCTION

In plasma-immersion ion implantation, a target immersed in a plasma is pulsed repetitively with large negative voltages. When the pulse is applied, electrons are repelled from the target on the time scale of the inverse electron plasma frequency, creating a uniform ion sheath. The ions, on a longer time scale, are attracted and implanted into the surface of the target. As the ions are implanted, the ion density in the sheath drops. This causes the sheath-plasma edge to recede and uncover more ions to increase the ion density in the sheath and sustain the potential drop across the sheath. The velocity of the moving sheath edge depends upon, among other factors, the pressure of the background neutral gas. Here, we develop a general one-dimensional model to study this process in different geometries for the case in which the pressure of the neutral gas is high enough that the ion motion in the sheath can be assumed to be highly collisional. We obtain analytic expressions for normal ion velocity distribution $f(v_x)$, sheath motion $s(t)$, ion flux at the target $J(t)$, and other parameters of interest. We apply this general model to planar and spherical targets, and compare the analytic results with those obtained by simulation. The following analysis was inspired by the work of Lieberman,[1] and Scheuer and Shamin,[2] Scheuer and Emmert,[3,4] and Conrad *et al.*[5]

II. ASSUMPTIONS

At time $t = 0^+$, the potential at the target drops to $-V_0$. This negative potential forces the electrons away from the target, forming an ion sheath. The sheath-plasma edge r_s moves far enough away, as shown in Fig. 1(a), so that the potential drop across the sheath equals V_0. The ion density in the sheath, n_s, is still the same as that in the plasma, n_0. At this point, the ions in the sheath, starting at essentially zero velocity, are accelerated by the resultant electric field. However, before traveling far, the ions collide with the neutral particles and scatter or lose their energy. Since the ions suffer many collisions before reaching the target, located at $r = r_a$, the time-varying ion density at any point in the sheath is assumed to change more slowly than the ion transit time through the sheath. The assumptions for this model are the following.

(1) The electron motion is instantaneous (inertialess).

(2) Charge exchange is the dominant ion-neutral collision mechanism.

(3) The ion motion is highly collisional; hence, $s \gg \lambda_i$, where $s = r_s - r_a$ is the sheath thickness, and λ_i is the ion-neutral mean free path.

(4) The applied voltage V_0 is much larger than the electron temperature T_e; hence, $s \gg \lambda_D$, where λ_D is the Debye length. The plasma potential is also chosen as the reference potential, $\phi_{\text{plasma}} = 0$.

(5) The ion charge density in the sheath is uniform in space, but varying slowly in time, as seen in Fig. 1(b). This is seen experimentally in dc glow discharges[6] and is also seen in simulation (see Sec. V). Further, we assume this charge density to be constant during the ion transit time in the sheath.

(6) In order to sustain a constant potential drop across the sheath, the ion loss at the target (the implanted ion current) is compensated by the uncovering of ions at the moving plasma sheath edge.

(7) Ions, having undergone many collisions with the neutrals in the plasma, enter the sheath at the neutral temperature (room temperature).

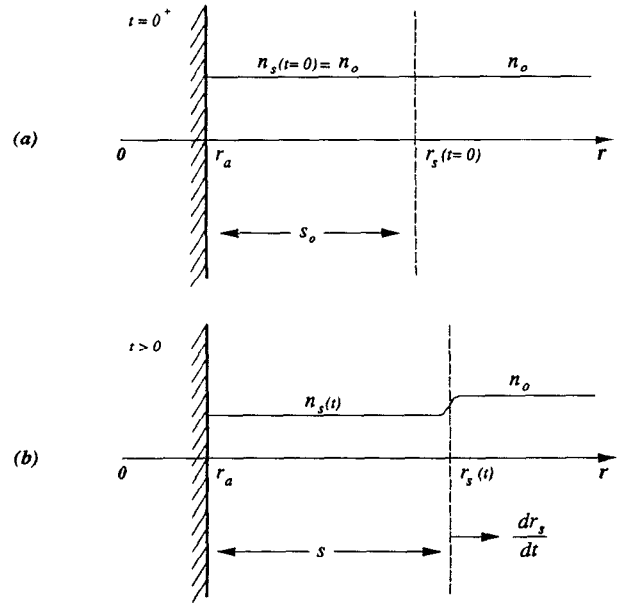

FIG. 1. The ion charge density in the sheath and sheath edge at time $t = 0^+$ and $t > 0$.

[a] Visiting from INPE, P. O. Box 515, S. J. dos Campos, SP, 12201, Brazil, supported partially by CAPES-Ministry of Education, Brazil.

 0021-8979/91/042008-07$03.00

III. ONE-DIMENSIONAL ANALYSIS

Assuming constant ion charge density in the sheath region $n_i = n_s$ (with $n_e = 0$), one can apply Gauss' law:

$$\nabla \cdot \mathbf{E} = \frac{e}{\epsilon_0} n_s, \tag{1}$$

with a boundary condition $E_r(r_s) \approx 0$ to get $E_r(r)$ (r is a general one-dimensional coordinate). Having found the electric field in the sheath, the electric potential can be obtained from $\nabla\phi = -\mathbf{E}$. The boundary condition at the target states that $\phi(r_a) = -V_0$ when the pulse is applied.

Now let us assume an ion, after suffering a charge-exchange collision with a neutral, starts from the rest at $r = r_0$, as seen in Fig. 2. This ion is accelerated by $E_r(r)$, normal to the target, according to the one-dimensional equation of motion

$$\ddot{r} = \frac{e}{M} E_r(r). \tag{2}$$

This acceleration occurs in planar, cylindrical, and spherical coordinates since we assume that the total ion velocity has dropped to near zero after the charge-exchange collision; hence, conservation of angular momentum forces the other velocity components to remain zero after the collision.

Equation (2) can be integrated with the following substitutions:

$$\dot{r} = u_r,$$

$$\ddot{r} = \frac{du_r}{dt} = \frac{du_r}{dr} u_r.$$

This gives

$$\frac{du_r}{dr} u_r = \frac{e}{M} E_r(r),$$

or

$$u_r^2(r,r_0) = 2\frac{e}{M}\int_{r_0}^{r} E_r(r)dr. \tag{3}$$

The velocity of the ion at the target, $r = r_a$, starting at r_0 is then

$$u_a = u_r(r_a, r_0), \tag{4}$$

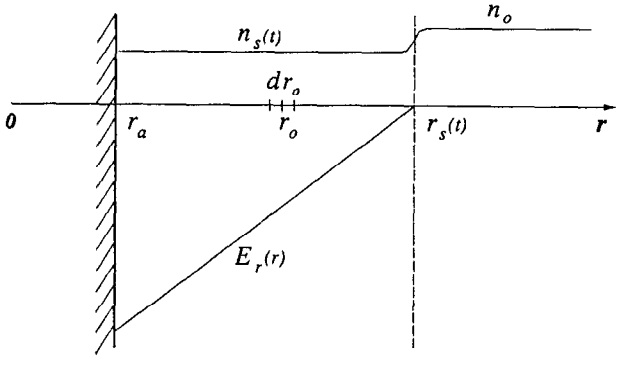

FIG. 2. An ion is assumed to be accelerated from rest at $r = r_0$ after a charge-exchange collision. The electric field shown is typical in the planar coordinates.

assuming the ion does not collide with a neutral again before reaching the target.

We now can get an expression for $f(u_a)$, the normal ion velocity distribution, by applying the condition for conservation of particles:

$$f(u_a)du_a = \exp\left(-\frac{r_0 - r_a}{\lambda_i}\right) n_s A(r_0) dr_0,$$

where $A(r_0)$ is the cross-sectional area at r_0, λ_i is the ion-neutral mean free path, and dr_0 is as shown in Fig. 2. The exponential factor, containing the neutral pressure dependence, is the probability of an ion, starting from rest at r_0, striking the target without suffering a charge-exchange collision. Thus, we have

$$f(u_a) = c_1 \exp\left(-\frac{r_0 - r_a}{\lambda_i}\right) n_s A(r_0) \frac{dr_0}{du_a}, \tag{5}$$

where dr_0/du_a is calculated from (4) and c_1 is determined by normalization.

Having calculated the ion velocity distribution, one can compute the average ion velocity at the target from

$$\bar{u}_a = \int u_a f(u_a) du_a. \tag{6}$$

The average ion current density at the target is then given by $J_a = \overline{en_a u_a}$, which is

$$J_a = en_s \bar{u}_a, \tag{7}$$

where the bar denotes average value over the velocity distribution and the ion density at the target, n_a, is assumed to be the same as in the sheath.

Noting that $\int_s \mathbf{J}\cdot d\mathbf{s} + (\partial/\partial t)\int_V \rho\, dV = 0$ guarantees conservation of charge, the sheath motion can be calculated from

$$J_a A(r_a) = -\frac{\partial}{\partial t}\left[en_s V(r_s, r_a)\right] + \frac{\partial}{\partial t}\left[en_0 V(r_s)\right], \tag{8}$$

where $V(r_s, r_a)$ is the volume of the sheath region and $\partial V(r_s)$ is the volume of the shell at r_s uncovered by the moving sheath edge over the interval ∂t. The first term in the right-hand side of (8) is the rate of change of the total ion charge in the sheath. This rate of change is zero if there is no charge accumulation in the sheath region; i.e., the ion density in the sheath, n_s, decreases at the same rate that the volume of the sheath region increases. The second term in the right-hand side of (8) is the rate at which the ions in the plasma are uncovered by the moving sheath edge, as shown in Fig. 1(b). This is the rate at which the ions are introduced into the sheath region, which must be the same as the ion loss at target if there is no charge accumulation in the sheath.

The parameters J_a, n_s, $V(r_s, r_a)$, and $V(r_s)$ in Eq. (8) are implicit functions of the sheath edge r_s. Hence, Eq. (8) can be integrated for $r_s(t)$. This could then be used to determine the time dependence of such parameters as J_a and $\bar{u}_a$. $J_a(t)$ represents the rate of ions implanted into the target per unit time, which is an important parameter in the ion implantation process.

IV. PLANAR COORDINATE SYSTEM

For simplicity, in this case one can assume that the target is located at the origin, $r_a = 0$; hence, $r_s = s$. In one-dimensional planar geometry, (1) becomes

$$\frac{\partial E}{\partial x} = \frac{en_s}{\epsilon_0}.$$

Integrating this from the sheath edge to some arbitrary position in the sheath, x, and assuming that $E(s) = 0$, we have

$$E(x) = \frac{en_s}{\epsilon_0}(x - s).$$

The electric potential with respect to the plasma potential is then

$$\phi(x) = \frac{en_s}{\epsilon_0}\left(sx - \frac{x^2}{2} - \frac{s^2}{2}\right).$$

Applying the boundary condition $\phi(0) = -V_0$, we obtain

$$n_s = \frac{2\epsilon_0 V_0}{es^2}. \tag{9}$$

Thus, the equation of motion for an ion starting from rest at $x = x_0$ after a charge-transfer collision in the sheath is

$$\frac{d^2x}{dt^2} = \frac{eE(x)}{M} = \frac{2eV_0}{Ms^2}(x - s),$$

where s, the sheath thickness, is assumed to vary slowly compared with the ion transit time. Integrating this using (3), we find

$$u^2 = \frac{u_m^2}{s^2}\left[(x^2 - x_0^2) - 2s(x - x_0)\right],$$

where $u_m^2 = 2eV_0/M$ is the square of the maximum ion velocity at the target. The ion velocity at the target is then given by

$$u_a^2 = \frac{u_m^2}{s^2}(2sx_0 - x_0^2). \tag{10}$$

Equation (5) in this case becomes

$$f(u_a) = c_2 e^{-x_0/\lambda_i} n_s A(x_0)\frac{dx_0}{du_a}.$$

Solving (10) for x_0 and differentiating x_0 with respect to u_a,

$$f(u_a) = \frac{c_2 u_a}{(1 - u_a^2/u_m^2)^{1/2}} \times \exp\left\{\frac{s}{\lambda_i}\left[\left(1 - \frac{u_a^2}{u_m^2}\right)^{1/2} - 1\right]\right\}.$$

The parameter c_2 is determined by normalization to be

$$c_2 = \frac{s}{\lambda_i u_m^2 (1 - e^{-s/\lambda_i})}.$$

The complete expression for $f(u)$ is therefore

$$f(u_a) = \frac{su_a}{\lambda_i u_m^2 (1 - e^{-s/\lambda_i})(1 - u_a^2/u_m^2)^{1/2}} \times \exp\left\{\frac{s}{\lambda_i}\left[\left(1 - \frac{u_a^2}{u_m^2}\right)^{1/2} - 1\right]\right\}. \tag{11}$$

Assuming $s \gg \lambda_i$, the average ion velocity at the target can be found using (6) to be

$$\bar{u}_a = \left(\frac{eV_0\pi\lambda_i}{Ms}\right)^{1/2}. \tag{12}$$

Inserting (12) and (9) into (7), we get

$$J_a = \epsilon_0\left(\frac{4\pi e\lambda_i}{M}\right)^{1/2}\frac{V_0^{3/2}}{s^{5/2}}. \tag{13}$$

The current density given by (13) has the same dependence on s and λ_i as the equation obtained by Lieberman,[7] but is greater by roughly a factor of 3. Lieberman uses $\mu = 2e\lambda_i/\pi Mu$ for the mobility of the ions in the sheath; this mobility is valid for the case in which ions are moving in a constant uniform applied electric field.[8] The electric field in the sheath is not constant; hence, the expression for the average mobility has a different coefficient.

In planar geometry, the term $n_s V(r_s, r_a)$ in Eq. (8) is time invariant; hence,

$$J_a = en_0\frac{ds}{dt}.$$

Thus the sheath velocity is

$$\frac{ds}{dt} = \frac{\epsilon_0}{en_0}\left(\frac{4\pi e\lambda_i}{M}\right)^{1/2}\frac{V_0^{3/2}}{s^{5/2}},$$

or

$$\frac{ds}{dt} = u_0\frac{s_0^{5/2}}{s^{5/2}}, \tag{14}$$

where $s_0 = (2\epsilon_0 V_0/en_0)^{1/2}$ is the initial sheath thickness, and $u_0 = (eV_0\pi\lambda_i/Ms_0)^{1/2}$ is a characteristic ion velocity in the sheath. Integrating (14), we find

$$s(t) = s_0(1 + \omega_0 t)^{2/7}, \tag{15}$$

where $\omega_0 = (7u_0/2s_0)^{1/2}$ is a characteristic frequency for the ions in the sheath.

Putting (15) into (9), (12), and (7), we obtain

$$n_s(t) = \frac{n_0}{(1 + \omega_0 t)^{4/7}}, \tag{16}$$

$$\bar{u}_a(t) = \frac{u_0}{(1 + \omega_0 t)^{1/7}}, \tag{17}$$

$$J_a(t) = \frac{en_0 u_0}{(1 + \omega_0 t)^{5/7}}. \tag{18}$$

One can also insert (15) into (11) to obtain the velocity distribution of ions as a function of time.

V. COMPARISONS WITH SIMULATION

We use the code PDP1[9,10] to simulate a one-dimensional planar-bounded plasma system. The particle-in-cell method, covered in detail by Birdsall and Langdon,[11] is implemented in PDP1 to solve for the particle and field parameters self-consistently. The code also uses a Monte Carlo scheme to model the collisions of charged and neutral particles (charge-exchange and scattering ion-neutral collisions, and elastic, excitation, and ionization electron-neutral collisions) with laboratory cross sections used to determine $\nu(E)$. In order to compare the analytic results [Eqs. (11),

(17), and (18)] with the simulation, we need only consider ion-neutral charge-exchange collisions.

At time $t = 0$, a pulse with a fall time of 1 μs and magnitude 500 V is applied to the left electrode, and the potential at the electrode is kept at this constant value thereafter. Initially, the space between the two electrodes is filled with a uniform plasma. The neutral gas used for these runs is argon, and the other common parameters are as follows: length = 30 cm, area = 100 cm^2, $n_0 = 10^7$ cm^{-3}, $V_0 = -500$ V, fall time = 1 μs, and $T_e = 1$ eV. The initial sheath thickness for these parameters is $s_0 = 7.43$ cm.

Note that the fall time of the voltage applied to the target is zero in the analytic treatment and is chosen to be 1 μs in the simulation. For the simulation case, the electron plasma frequency f_p in the bulk plasma is given by $f \approx 9000\sqrt{n(\mathrm{cm}^{-3})} = 28$ MHz. To avoid plasma oscillation excitation, $1/T_f$ (T_f = fall time) should be well below the plasma frequency. For $T_f = 1$ μs, this condition is satisfied, and no plasma oscillation is observed in the simulation. However, the fall time should also be less than the characteristic ion transit time in the sheath, $T = \omega_0^{-1}$, to get a reasonable comparison with the theory. The characteristic ion transit time in the sheath is calculated, for the analytic case, to be roughly 1.5 μs at 20 mTorr and larger at higher pressures. Although the ion transit time in the sheath seems to be on the order of the fall time, the applied voltage in the simulation is falling over this entire time interval. Hence, the average voltage applied to the target is lower than the final voltage, and the average sheath motion is slower. This suggests that the effect of shortening the fall time will not significantly change the dynamics. To test this, we ran the simulation with $T_f = 0.5$ μs, and no significant change was observed.

The comparisons are made at the neutral pressures of 20, 30, 50, and 100 mTorr. For these pressures, the ratios of the initial sheath thickness to the ion-neutral mean free path, s_0/λ_i, are, respectively, 18, 27, 45, and 90.

Figure 3 shows the ion and electron number densities at time $t = 1$ μs, when the pulse is fully applied, and a later time

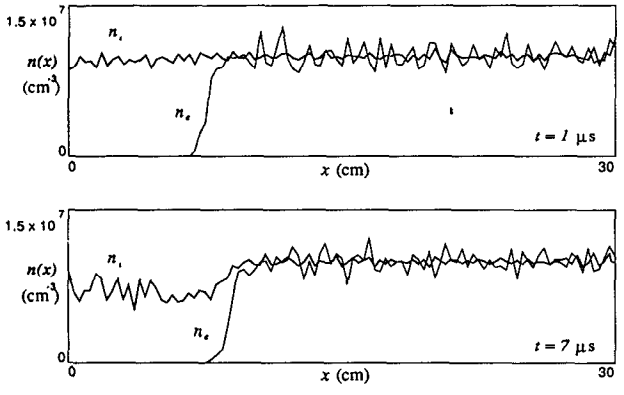

FIG. 3. A simulation output showing the ion and electron densities in the planar geometry. At $t = 1$ μs, the potential at the left electrode is V_0, the sheath edge has moved to its initial position, and the ion density in the sheath appears to be roughly the same as that in the plasma. At $t = 7$ μs, the sheath edge has moved farther away from the electrode, and the ion density in the sheath has a nearly uniform profile.

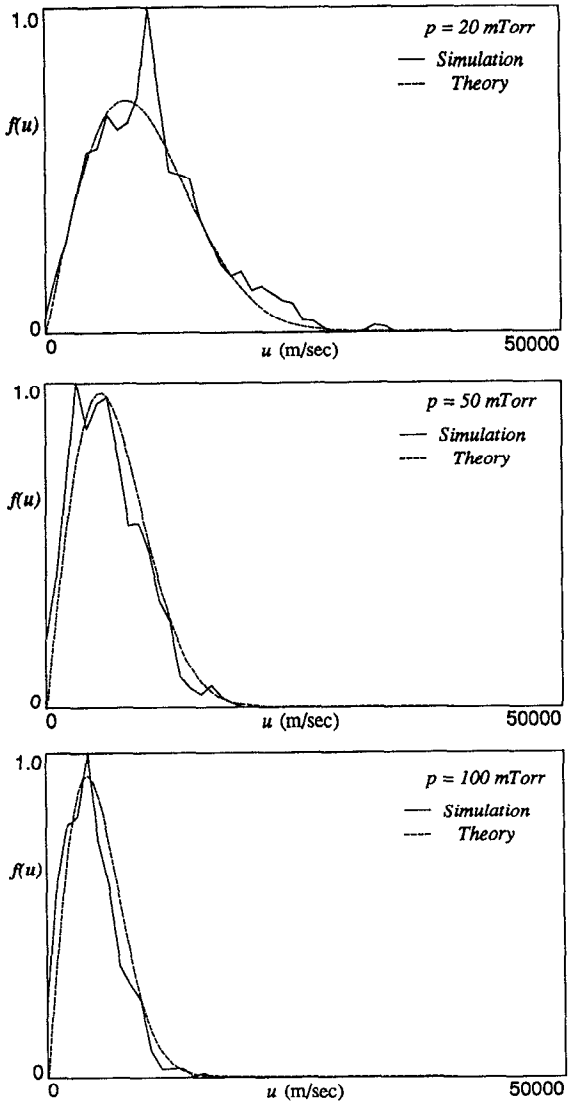

FIG. 4. Ion velocity distribution at the planar target. Note that the maximum ion velocity at the target, $u_m = (2eV_0/M)^{1/2}$, is roughly 50 000 m/s for this applied voltage.

$t = 7$ μs for the neutral pressure of $p = 50$ mTorr. These density profiles tend to justify our assumption of uniform ion density in the sheath.

As previously described, one can put (15) into (11) to get the instantaneous velocity distribution of ions. Doing so, we compare the result with the simulation at the following pressures: $p = 20$, 50, and 100 mTorr, as seen in Fig. 4. The analytic expression for the instantaneous distribution function at 20, 50, and 100 mTorr is evaluated, respectively, at the following times: $t = 80$, 69, and 64 μs.

Figure 5 displays a comparison of Eq. (17), average ion velocity at the target as a function of time, with a simulation for the neutral pressures of 20 and 30 mTorr.

Equation (18), the ion flux at the target as a function of time, is compared in Fig. 6 with simulation for the neutral pressures of 50 and 100 mTorr. Although the ion flux compares well with the simulation, the analytic average ion velocity appears to be somewhat smaller than the one obtained by simulation. The discrepancy may come from the constant

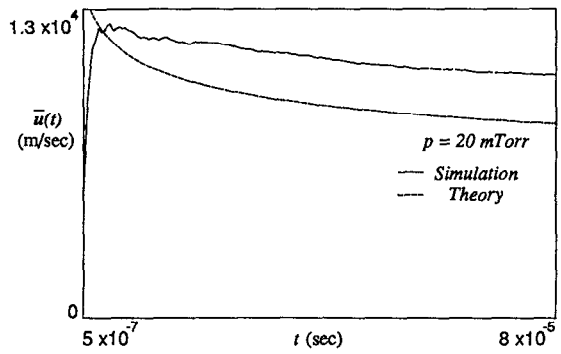

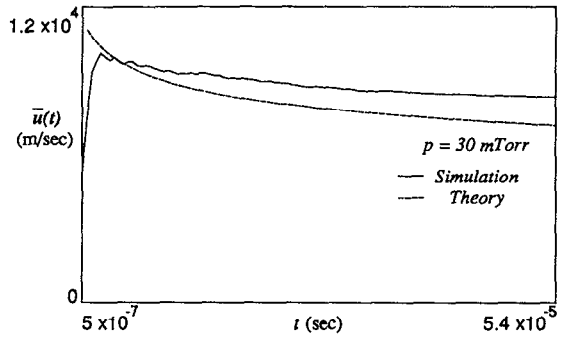

FIG. 5. A linear plot of the time response of average ion velocity at the target in the planar geometry.

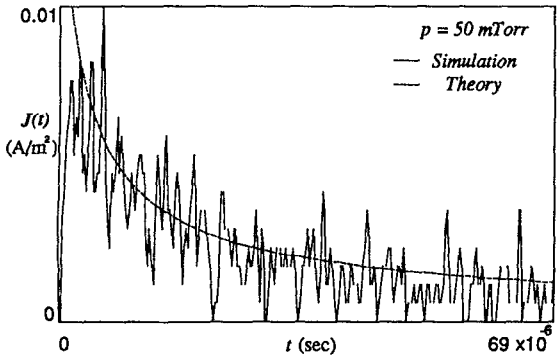

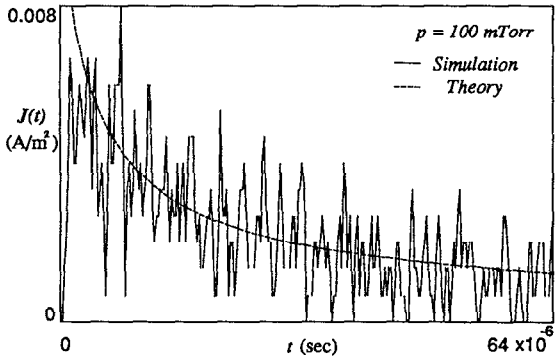

FIG. 6. The time response of ion current density at the planar target (linear plot).

profile assumed for the ion density in the sheath. The ion density seen in the simulation is not quite uniform, being slightly lower at the target.

VI. SPHERICAL COORDINATE SYSTEM

In this geometry, we assume the target to be a sphere of radius r_a; hence, (1) becomes

$$\frac{1}{r^2}\frac{\partial}{\partial r}(r^2 E_r) = \frac{en_s}{\epsilon_0}.$$

One can integrate this from the sheath edge r_s to some r in the sheath to obtain

$$E_r(r) = \frac{en_s}{3\epsilon_0}\left(r - \frac{r_s^3}{r^2}\right),$$

provided $E_r(r_s) = 0$. The electric potential with respect to the plasma potential is then

$$\phi(r) = -\frac{en_s}{3\epsilon_0}\left(\frac{r^2}{2} + \frac{r_s^3}{r} - \frac{3}{2}r_s^2\right).$$

Applying the boundary condition $\phi(r_a) = -V_0$, we get

$$n_s = \frac{6V_0\epsilon_0 r_a}{eR^3}, \tag{19}$$

where

$$R^3 = r_a^3 + 2r_s^3 - 3r_s^2 r_a.$$

At time $t = 0$, the density in the sheath is assumed to be the same as in the bulk plasma. Hence, the initial position of the sheath edge can be found from (19) to be

$$r_{s_0} \approx (3r_a V_0\epsilon_0/en_0)^{1/3} + r_a/2.$$

This expression is the same as that derived by Conrad[12] plus a correction term $r_a/2$ for the case in which r_s is comparable to r_a.

We will carry on the analysis assuming $r_s \gg r_a$, where the electric field can be approximated by

$$E_r(r) \approx -\frac{en_s}{3\epsilon_0}\left(\frac{r_s^3}{r^2}\right),$$

and R^3 reduces to

$$R^3 \approx 2r_s^3. \tag{20}$$

Equation (2) in this case becomes

$$\ddot{r} = -\left(\frac{e^2 n_s}{3\epsilon_0 M}\right)\frac{r_s^3}{r^2}.$$

Integrating this, using (3), we get

$$u^2 = r_a u_m^2\left(\frac{1}{r} - \frac{1}{r_0}\right),$$

where $u_m^2 = (2eV_0/M)(2r_s^3/R^3)$ is the square of the maximum ion velocity at the target modified by a scaling factor due to the geometry. The ion velocity at the target is then

$$u_a^2 = r_a u_m^2\left(\frac{1}{r_a} - \frac{1}{r_0}\right). \tag{21}$$

Equation (5) in this coordinate system becomes

$$f(u_a) = c_3 \exp\left(-\frac{r_0 - r_a}{\lambda_i}\right) r_0^2 \frac{dr_0}{du_a}.$$

Solving for r_0 in (21) and differentiating it with respect to u_a,

$$f(u_a) = c_3 \frac{u_a/u_m}{[1-(u_a/u_m)^2]^4} \times \exp\left(-\frac{r_a}{\lambda_i}\frac{(u_a/u_m)^2}{1-(u_a/u_m)^2}\right).$$

The constant c_3 is determined by normalization to be

$$c_3 = \frac{2r_a^3}{u_m(\lambda_i r_a^2 + 2\lambda_i^2 r_a + 2\lambda_i^3)}.$$

For $r_a \gg \lambda_i$,

$$c_3 \approx \frac{2r_a}{u_m \lambda_i}.$$

Putting this value into the expression for $f(u)$,

$$f(u_a) = \frac{2r_a}{u_m\lambda_i}\frac{u_a/u_m}{[1-(u_a/u_m)^2]^4} \times \exp\left(-\frac{r_a}{\lambda_i}\frac{(u_a/u_m)^2}{1-(u_a/u_m)^2}\right). \quad (22)$$

The average ion velocity at the target, given by (6), is then

$$\bar{u}_a = \left(\frac{r_2^3}{R^3}\right)^{1/2}\left(\frac{eV_0\pi\lambda_i}{Mr_a}\right)^{1/2}. \quad (23)$$

Inserting Eqs. (23) and (19) into Eq. (7),

$$J_a = \epsilon_0\left(\frac{36\pi e r_a\lambda_i}{M}\right)^{1/2}\frac{V_0^{3/2}}{r_s^3}\left(\frac{r_s^3}{R^3}\right)^{3/2}. \quad (24)$$

Using Eq. (8) to determine the motion of sheath edge in this geometry and noting that the term $n_s V(r_s, r_a)$ is time invariant for $r_s \gg r_a$, we have

$$4\pi r_a^2 J_a = 4\pi r_s^2 e n_0 \frac{dr_s}{dt},$$

which, assuming $r_s \gg r_a$ and using (20), can also be written as

$$\frac{dr_s}{dt} = \frac{u_0 r_a^2 r_{s_0}^3}{r_s^5}, \quad (25)$$

where $r_{s_0}^3 = (3V_0\epsilon_0 r_a/en_0)$ is the initial position of the sheath edge, and $u_0 = (eV_0\pi\lambda_i/2Mr_a)^{1/2}$ is a characteristic ion velocity in the sheath. Equation (25) can be integrated to find r_s as a function of time to be

$$r_s = r_{s_0}(1+\omega_0 t)^{1/6}, \quad (26)$$

where $\omega_0 = 6u_0 r_a^2/r_{s_0}^3$ is a characteristic ion frequency in the sheath.

One can put Eq. (26) into Eqs. (19), (23), and (7) to obtain

$$n_s(t) = \frac{n_0}{(1+\omega_0 t)^{1/2}}, \quad (27)$$

$$\bar{u}_a(t) = u_0, \quad (28)$$

$$J_a(t) = \frac{en_0u_0}{(1+\omega_0 t)^{1/2}}. \quad (29)$$

Even when r_s is comparable to r_a, Eqs. (26)–(29) may be used to approximate the sheath dynamics. One can also obtain the velocity distribution of ions as a function of time by inserting (26) into (22).

VII. COMPARISONS WITH SIMULATION

The code PDS1[13] is used in this case to simulate a one-dimensional spherically bounded plasma system. This code is the same as PDP1 with the basic difference that the field parameters and equations of motion are solved in the spherical coordinates. This code also uses a Monte Carlo scheme to model the collisions of charged and neutral particles, and again we need only consider ion-neutral collisions to compare the analytic results with the simulation. In this case we will compare Eq. (11) with the simulation running with argon as the background neutral gas and the following parameters: $r_a = 1$ cm, $p = 50$ mTorr, $n_0 = 10^7$ cm^{-3}, $V_0 = -10\,000$ V, fall time $= 1\,\mu$s, and $T_e = 1$ eV.

For these parameters, the ion-neutral mean free path, initial position of the sheath edge, average ion velocity, and the characteristic ion frequency and period in the sheath are calculated to be, respectively, $\lambda_i = 0.164$ cm, $r_{s_0} = 11.8$ cm, $u_0 = 7.86\times10^4$ m/s, $\omega_0 = 2.87\times10^4$ Hz, and $T = \omega_0^{-1} = 3.5\times10^{-5}$ s.

Figure 7 shows a reasonable agreement between theory and simulation for the distribution function. The analytic expression for the distribution is evaluated at $t = 70\,\mu$s. Note that at this pressure, the ratio of the initial sheath thickness to the ion-neutral mean free path, s_0/λ_i, is roughly 66.

Equation (28), the average ion velocity at the target as a function of time, is compared in Fig. 8 with the simulation. The simulation also suggests that the average ion bombardment energy at the spherical target, with $r_s \gg r_a$, is time invariant in contrast to the time-variant result obtained for the planar target [Eq. (17), Fig. 5].

The ion charge accumulation in the target as a function of time, $Q_a(t)$, is obtained by integrating Eq. (29):

$$Q_a(t) = \int_0^t J_a(t)dt.$$

This analytic result was calculated, compared with the simulation, and shown to be smaller by roughly a factor of 2. The disagreement may be a result of the assumption of a constant profile for the ion charge density in the sheath. The observed

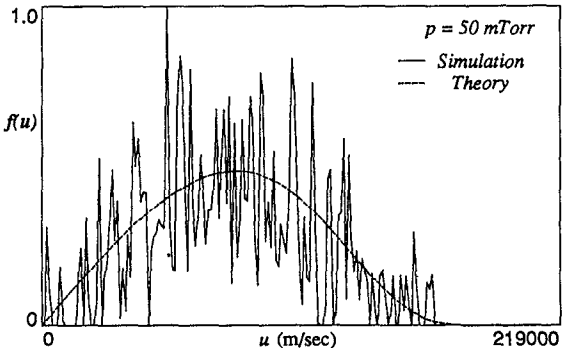

FIG. 7. Ion velocity distribution at the target in the spherical coordinate system.

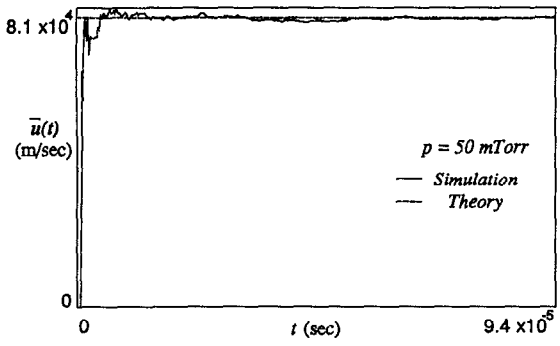

FIG. 8. A linear plot of average ion velocity at the spherical target as a function of time.

ion charge density from the simulation is not quite uniform, being slightly higher at the target, unlike what was seen for the planar target.

VIII. SUMMARY

A one-dimensional collisional model has been developed to study plasma-immersion ion implantation in the high-pressure regime. The model describes the sheath expansion as a function of time, ion velocity distribution at the target, and the ion flux at the target as a function of time. The problem is solved in both planar and spherical coordinate systems, and the analytic results compare well with those obtained by simulation.

ACKNOWLEDGMENTS

This work was supported in part by ONR Contract No. N00014-90-J-1198, NFS Grant No. ECS-8517363, DOE Grant No. DE-FG-03-87ER13727, a gift from Applied Materials, Inc., and a State of California MICRO Grant.

[1] M. A. Lieberman, J. Appl. Phys. **66**, 2926 (1989).
[2] J. T. Scheuer, M. Shamim, and J. R. Conrad, in *Proceedings of the 42nd Annual Gaseous Electronics Conference,* Palo Alto, 1989, Vol. NA-12, p. 166.
[3] J. T. Scheuer and G. A. Emmert, Phys. Fluids **31**, 3645 (1988).
[4] J. T. Scheuer and G. A. Emmert, Phys. Fluids **31**, 1748 (1988).
[5] J. Conrad, J. Radtke, R. Dodd, and F. Worzala, J. Appl. Phys. **62**, 4951 (1987).
[6] M. N. Hirsh and H. J. Oskam, *Gaseous Electronics* (Academic, New York, 1978), Vol. I.
[7] M. A. Lieberman, J. Appl. Phys. **65**, 4186 (1989).
[8] B. M. Smirnov, *Physics of Weakly Ionized Gases* (Mir, Moscow, 1981).
[9] I. J. Morey, V. Vahedi, and J. Verboncoeur, Bull. Am. Phys. Soc. **34**, 2028 (1989).
[10] Codes available from Industrial Liaison Program, EECS Dept., UC Berkeley, CA 94720.
[11] C. K. Birdsall and A. B. Langdon, *Plasma Physics Via Computer Simulation* (McGraw-Hill, New York, 1985).
[12] J. R. Conrad, J. Appl. Phys. **62**, 777 (1987).
[13] M. A. Alves, V. Vahedi, and C. K. Birdsall, Bull. Am. Phys. Soc. **34**, 2028 (1989).